

Numerical analysis for the coating thickness prediction in continuous hot-dip galvanizing[†]

Soon-Bum Kwon^{1,*}, Young-Doo Kwon¹, Sung-Jin Lee¹, Seung-Young Shin¹,
and Geun-Young Kim²

¹*School of Mechanical Engineering, Kyungpook National University, 1370, Sankyuk-dong, Daegu 702-701-, Korea*

²*POSCO Technical Research laboratories 699, Gumgo-dong, Jeonnam 545-090, Korea*

(Manuscript Received October 13, 2008; Revised July 3, 2009; Accepted September 10, 2009)

Abstract

Gas wiping is a decisive operation in the hot-dip galvanizing process. Especially, it has a crucial influence on the thickness and uniformity of coating film, but may be subsequently responsible for splashing. To date, the number of fundamental studies on the jet structure impinging on a vertical moving strip for various nozzle systems has not been sufficient to draw any meaningful conclusion. In this connection, at first, to confirm the validation of numerical analysis, the impinging jet pressure on the surface of a vertical strip by experiment is compared with the results by numerical analysis. Next, after confirming for the superiority of a constant expansion rate nozzle in splashing, the relationship between the stagnation pressure and the impinging jet pressure distribution issuing from the nozzle system of constant expansion rate is investigated. Finally, by using the calculated wall shear stress, the relationships among the coating thickness, strip speed and nozzle stagnation pressures are clarified. It is found that the impinging wall pressure for the case of constant expansion rate nozzle is more favorable for the problem of splashing to the case of the conventional one. Furthermore, from the point of view of energy conservation, it is advisable to use a constant expansion rate nozzle as a gas-wiping nozzle.

Keywords: At coating thickness; Continuous hot-dip galvanizing; Expansion rate; Gas wiping; Numerical analysis

1. Introduction

It has been known from early days that an advantage of gas wiping in the hot-dip galvanizing process is the ease of controlling the film coating thickness and guaranteeing the uniformity in coating thickness with a fast galvanizing speed [1, 2].

In general, the key issue in the continuous hot-dip galvanizing process is the ability to produce steel strip with the coating weight specified by a customer at the highest possible line speed. Nowadays, a typical furnace allows the production of about 65 tons of steel

per hour, which implies 3.3 m/s. in a maximum line speed for a 0.7 mm thick/1m width of strip [3]. So, to cope with the demands of the speed-up of a galvanizing line obtaining the same film thickness with a conventional system, it is inevitable that the stagnation settling chamber pressure of the nozzle is increased or the gap from the nozzle lip to the strip surface is shortened. However, the increase of nozzle stagnation pressure and the shortening of the impinging gap between the nozzle lip and the strip surface may cause a problem of splashing for certain line speeds typically above 2.5 m/s [4].

Since the splashing phenomenon is a physical limitation of the gas wiping process, it cannot be thoroughly suppressed, but it has been revealed that it can be diminished to some extent by the optimal design of the air-knife nozzle [5]. Because the splashing is

[†] This paper was recommended for publication in revised form by Associate Editor Jun Sang Park

*Corresponding author. Tel.: +82 53 950 5578, Fax.: +82 53 950 6550

E-mail address: sbkwon@knu.ac.kr

© KSME & Springer 2009

caused intrinsically by the separation of the running back liquid film, it is very important to know exactly the distribution of impinging pressure and the jet structure at the junction of the strip surface.

In general, the flow expanded through a conventional nozzle may lead to undulations in the pressure distribution [6]. And such a parasitic undulation of the flow can stir up the onset of splashing, and can cause the deterioration of coating quality and can also lead to the larger consumption of energy in the gas wiping process. With respect to these connections, in the present study, three kinds of nozzles having a constant expansion rate [6] for galvanizing gas wiping were designed, and the results through the constant expansion rate nozzle are compared with the results through the conventional one. In comparison, to cope effectively with the harmful problem of splashing, the distribution of impinging wall jet pressure with the variations of stagnation settling chamber pressure(p_0) was investigated, and also by using the results of calculated wall shear stress the distribution of zinc coating thickness with p_0 for each nozzle system was calculated.

2. Experimental set-up

To confirm the validation of the numerical method used, the distribution of the impinging wall jet pressure on a vertical plate by experiment is compared with the results by numerical analysis. In the current experiment, the wall impinging pressures along the center-plane of the vertical plate are measured by a 16-channel scanning valve system(model; DSA-3017) connected to semi-conductor pressure transducers with intervals of 1 mm in zigzagging as shown in Fig. 1. Also, to measure more densely the impinging wall pressure along the jet center-plane, a 3 axis auto-traverse unit whose measuring interval is 0.25 mm was used. Here, to minimize the fluttering of the vertical plate caused by impingement of the jet, the thickness of the steel plate is 10 mm, and the out diameter of the static hole to measure the static pressure is 0.8 mm, respectively. Fig. 1 shows the schematic of the experimental set-up. And Fig. 2 shows the details of the new designed nozzles whose expansion rate of the nozzle(that is, $-\frac{1}{p} \frac{dp}{dt}$) is constant at $88,000 \text{ s}^{-1}$ and a

conventional nozzle used in the actual field. Here, since the nozzle inlet and exit areas for all of the stagnation conditions are the same as those of the conventional

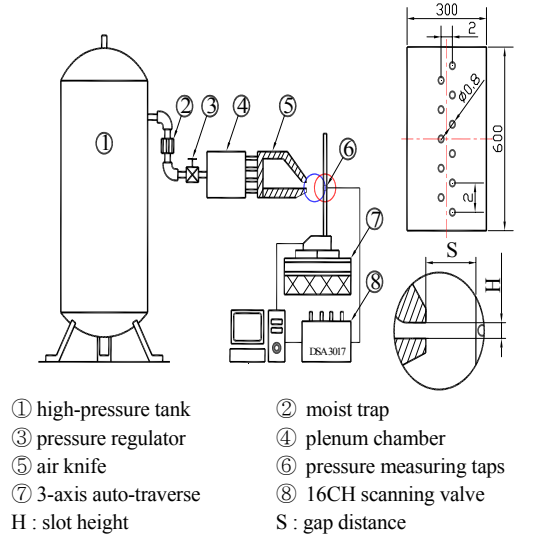


Fig. 1. Schematic of experimental set-up used in impinging wall jet pressure experiments.

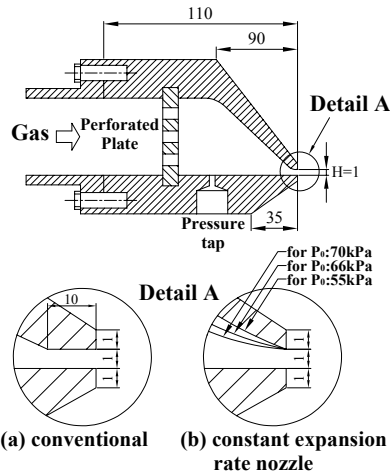


Fig. 2. Specification of nozzle system.

case, the differences in nozzle contour for various stagnation settling chamber conditions show up at the length between the inlet and exit of the nozzle and the contour of the nozzle inner wall, and the expansion rate of the nozzle corresponds to the case when an air of the stagnation condition of 55 kPa, 66 kPa or 70 kPa with the temperature of 300 K expands through the nozzle equipped with a perforated plate to the standard atmospheric condition.

3. Numerical analysis

In the gas wiping process of continuous hot-dip galvanizing, it is known that the performance of a

wiping system is mainly dependent on the impact pressure gradient and shear stress distribution of the impinging jet on the liquid surface, and both depend principally on the stagnation settling chamber pressure(p_0), the gap between the nozzle lip and vertical strip(S) and the nozzle slot height(H). In the present study, to clarify the effects of expansion rate of the nozzle and the speed of the strip on the distributions of impinging jet pressure and zinc coating thickness, the values of S and H are constant as 10 mm and 1 mm, respectively. And the working fluid for gas wiping is dehumidified compressed air.

Fig. 3 shows an analytical model of gas wiping. As is shown in the figure, in the case of calculating the coating thickness, it is necessary to calculate(or measure) exactly the shear stress acting on the boundary of the liquid film, but, since the film thickness is so thin, and there is no alternative in this stage to obtain the exact solution on shear stress, the wall shear stress, was used, as calculated from the numerical analysis as the shear stress acting on the boundary of the liquid film [7].

3.1 Calculation procedure for impinging jet

In the present computational work, the commercial code of Fluent 6.0 was used, in which the equations of continuity, two-dimensional time dependent Navier-Stokes, energy, state and so on are used as governing equations. In the calculation of dynamic viscosity of working fluid, and the equation suggested by Sutherland, the standard k-ε turbulent model to solve the turbulent stress was used in each case. The schematic computational domain and each boundary condition are shown in Fig. 4. The grid makes densely in the region which has the large possibility of change in pressure, velocity and so on, like the exit of an air knife. The numbers of mesh and mesh type are about 19 thousands and a tetragon, respectively. The working fluid is air, and it is assumed to be thermally and calorically perfect. Three kinds of settling chamber conditions, that is, the pressures and temperature at the downstream of the perforated plate, are constant to be 55 kPa, 66 kPa, 70 kPa and 300 K, respectively.

3.2 Calculation procedure for coating thickness

The numerical analysis to calculate the zinc coating thickness at the center-plane of the strip is based on the following basic assumptions: (1) it can be assumed

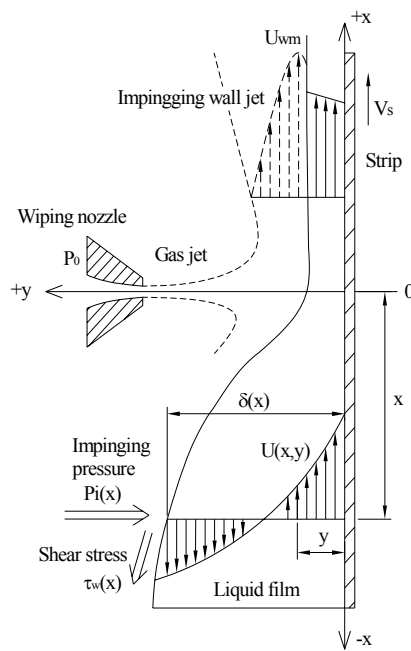


Fig. 3. Analytical model of gas wiping.

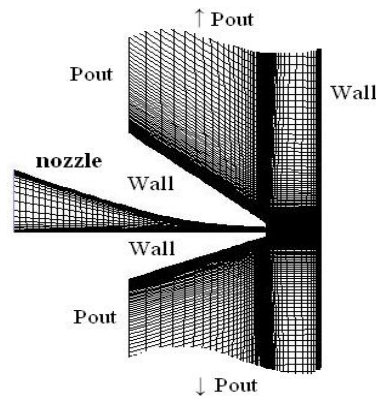


Fig. 4. Computational domains and boundary conditions.

that the fluid flow in the liquid coating layer is at a steady state, two-dimensional equations of incompressible, constant viscosity, creep flow, and (2) the surface tension effect of the liquid zinc can be neglected. Using the coordinate system shown in Fig. 3, the governing equations and boundary conditions can be summarized as follows.

Continuity and momentum equations:

$$\frac{\partial u}{\partial x} = 0 \tag{1}$$

$$u \frac{\partial u}{\partial x} = -\frac{1}{\rho_l} \frac{\partial p}{\partial x} - g + \frac{\mu_l}{\rho_l} \left(\frac{\partial^2 u}{\partial x^2} + \frac{\partial^2 u}{\partial y^2} \right) \tag{2}$$

Boundary conditions:

$$\begin{aligned}
 u(x, y)|_{y=0} &= V \\
 p(x)|_{y=\delta(x)} &= p_i(x) \\
 \mu_l \frac{\partial u(x, y)}{\partial y} \Big|_{y=\delta(x)} &= \tau_w(x)
 \end{aligned} \tag{3}$$

Here μ_l, ρ_l, V_s, p_i and τ_w represent dynamic viscosity, density of the zinc liquid, strip speed, wall impinging pressure and wall shear stress, respectively. Since the viscosity of molten zinc is relatively insensitive to temperature until the temperature falls within approximately 5°C of the freezing point, it is assumed that the viscosity of liquid zinc in the wiping zone is constant [8]. Also, because of the thin thickness of zinc liquid film (about 10 μm), it is assumed that the impinging jet pressure without liquid zinc film is equal to the value with liquid zinc film. In Table 1, the numerical and experimental conditions are tabulated.

By using the above governing equations and boundary conditions, the distribution of velocity in the liquid film can be found analytically.

$$\begin{aligned}
 u(x, y) &= V_s + \frac{\tau_w(x)}{\mu_l} - \frac{1}{\mu_l} \left(\frac{dp_i(x)}{dx} + \rho_l g \right) \\
 &\left(\delta(x) - \frac{y}{2} \right) y
 \end{aligned} \tag{4}$$

So, the volume flow rate per unit width of strip becomes

$$\begin{aligned}
 q &= \int_0^{\delta(x)} u(x, y) dy = V_s \delta(x) \\
 &+ \frac{\tau_w(x)}{2\mu_l} \delta^2(x) - \frac{1}{3\mu_l} \left\{ \frac{dp_i(x)}{dx} + \rho_l g \right\} \delta^3(x)
 \end{aligned} \tag{5}$$

Finally, the mean film thickness δ_m can be obtained as:

Table 1. Numerical and experimental conditions.

nozzle slot gap (H)	1.0 mm
nozzle-strip distance (S)	10.0 mm
strip speed (V _s)	2.5, 3.0 m/s
operating fluid	Air (27 °C)
nozzle pressure (p ₀)	50 ~ 70 kPa
density of molten zinc (ρ _l)	6,634 kg/m ³⁽⁹⁾
viscosity of molten zinc (μ _l)	3.04 × 10 ⁻³ Pa · s ⁽⁹⁾

$$\begin{aligned}
 \delta_m &= \frac{q}{V_s} = \delta(x) + \frac{\tau_w(x)}{2\mu_l V_s} \delta^2(x) - \frac{1}{3\mu_l V_s} \\
 &\left\{ \frac{dp_i(x)}{dx} + \rho_l g \right\} \delta^3(x)
 \end{aligned} \tag{6}$$

In which, to obtain the volume flow rate per unit width q (that is δ_m), the boundary condition was used at the coordinate origin ($\eta = 0$), that is, $\frac{\partial q}{\partial \delta} = 0$. And, because of excessively large differences among the values of each flow property, it is necessary to normalize the flow properties as follows [9].

$$\left. \begin{aligned}
 \delta_m^* &= \frac{\delta_m}{\sqrt{\frac{\mu_l V_s}{\rho_l q}}} \\
 \delta^*(\eta) &= \frac{\delta(\eta)}{\sqrt{\frac{\mu_l V_s}{\rho_l q}}} \\
 p_i^*(\eta) &= 1 + \frac{1}{\rho_l g b_p} \frac{dp_i(\eta)}{d\eta} \\
 \tau_w^*(\eta) &= \frac{\tau_w(\eta)}{\sqrt{\rho_l \mu_l g V_s}}
 \end{aligned} \right\} \tag{7}$$

Here, $\eta \equiv x/b$, and b is the half-width at the point where $p = p_{\max}/2$. [7], which can be obtained from the result of numerical analysis on the distribution of impinging wall jet pressure.

Finally, Eq. (6) can be rewritten as

$$\delta_m^* = \delta^*(\eta) \left\{ 1 + \frac{1}{2} \tau_w^*(\eta) \delta^*(\eta) - \frac{1}{3} p_i^*(\eta) \delta^{*2}(\eta) \right\} \tag{8}$$

As a consequence, the non-dimensional coating thickness $\delta_m^*(\eta)$ can be calculated by using the known values of δ_m^* , τ_w^* and p_i^*

4. Results and discussions

4.1 Comparison between numerical analysis and experimental results

At first, to confirm the validation of the used numerical analysis, for the experimental condition of $p_0 = 66$ kPa and $T_0 = 300$ K, the impinging wall pressure at the center-plane of the vertical plate for the case of constant expansion rate nozzle was measured by a 3-axis auto-traverse unit equipped with a scanning valve system, and was compared with the result by numerical analysis; its results for impinging wall pressure are shown in Fig. 5. Here, the solid lines

with a closed circle and a dotted line correspond to the cases for experiment and numerical analysis, respectively. And, it can be found that the position of the maximum impinging wall pressure is located at the slight downward direction from the origin by gravitational effect. As is shown in the figure, from the good agreement between the two results, the validation of the used numerical analysis method can be confirmed. Also, the validation of program for the calculation of coating thickness was confirmed by the comparison of result of numerical analysis with the result of field works in final coating thickness. For example, for the case of conventional air-knife system ($H=1.3$ mm, $S=4$ mm, $V_s=2.5$ m/s and $p_0=61$ kPa), the final coating thicknesses by the numerical analysis and field works are 5.3 and 5.6 μm , respectively. Despite the small discrepancy between both results, the coating thickness by numerical analysis well agreed with the result of field works in general. From this, it can be concluded that the validation of numerical method for the calculation of coating thickness is confirmed.

In the case of the fixed plate (that is, no moving strip), $p_0=66$ kPa and $\dot{P}=88,000$ s^{-1} , the distributions of impinging wall pressure for the nozzles of constant expansion rate nozzle and conventional one are shown in Fig. 6. As can be expected, for the same coating conditions, because of the undulation effects within the nozzle internal flow and the violent interaction between the flow and nozzle wall for the conventional nozzle, the maximum impinging wall pressure for the conventional nozzle is smaller than the case of the constant expansion rate one. And, due to the effect of gravity, the positions of the maximum impinging wall pressure for both cases deviate from the origin of the coordinate, that is, located at the slight downside from the origin.

Furthermore, in general, since the length of the potential core will affect directly the thickness of the zinc coating film, the potential core lengths with p_0 for the case of free jets are measured by using the numerical results. Here, the potential core length defined as the length, between the nozzle exit and the point of 99.0% of the nozzle maximum exiting velocity along the jet centerline was used in the calculation. As shown in Fig. 7, for the same p_0 , it can be found that the length of the potential core for the constant expansion rate nozzle is longer than that of the conventional system, which will result in the larger impinging wall pressure (that is, a larger wall shear stress). And the

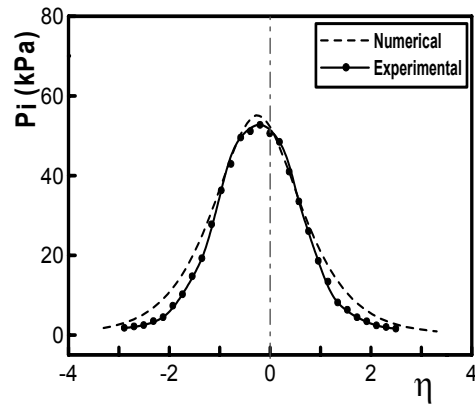


Fig. 5. Comparison between numerical analysis and experimental results of impinging wall jet pressure ($H=1.0$ mm, $S=10$ mm, $p_0=66$ kPa).

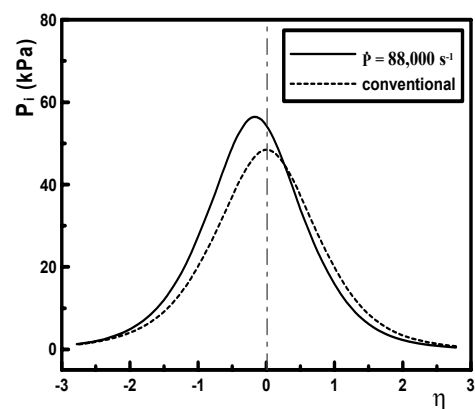


Fig. 6. Distributions of impinging wall pressure for constant expansion rate nozzle and conventional one ($H=1.0$ mm, $S=10$ mm, $V_s=0$, $p_0=66$ kPa).

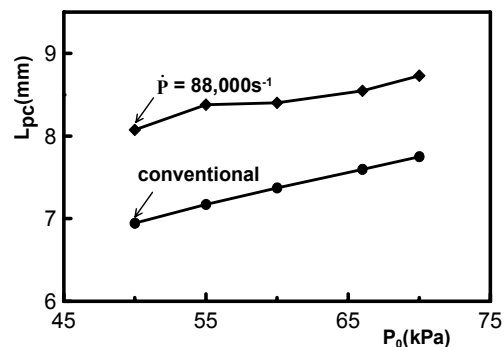


Fig. 7. Comparison of potential core lengths between constant expansion rate nozzle and conventional one with p_0 .

higher p_0 is, the larger the potential core length becomes. On the other hand, it can be found that the lengths of the potential core for both present nozzle systems are comparable to the lengths by Trentacoste et al [10].

Here, the symbols \blacklozenge and \bullet refer to the cases of constant expansion rate nozzle and conventional one, respectively. So, using a constant expansion rate nozzle system, it is possible to obtain the same coating thickness despite the lower stagnation settling chamber pressure or the higher strip speed. From the vantage point of energy consumption, it can be concluded that it is recommended to use the nozzle having a constant expansion rate for the air-knife system.

The characteristics of wiping jets with the variations of p_0 for $\dot{p}=88,000 \text{ s}^{-1}$ are shown in Fig. 8. Regardless of p_0 , the non-dimensional wall pressure gradient and shear stress, which will play a key role on the coating thickness, becomes maximum(or minimum) at the vicinity of the origin of the jet ($\eta=0$).

For the same coating condition excepting p_0 , it is found that the impinging wall pressure, which will affect directly the wall pressure gradient and shear stress, increases with the increase of p_0 .

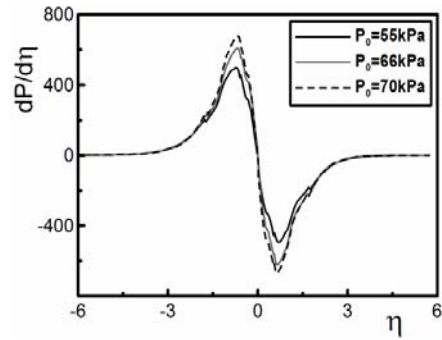
And, because of the relative velocity between the strip and air stream for the same p_0 and V_s , the maximum wall shear stress acting on the downside of the origin is slightly larger than that of the upper side of the origin; also, the place of zero wall shear stress is located at the slight downstream of the origin.

Fig. 9 shows the distributions of coating thickness of zinc by using the wall shear stress from the numerical analysis for the strip speed of 3.0 m/s. As can be expected, for the same coating conditions excepting the expansion rate of the nozzle, it turned out that the minimum coating thickness for the constant expansion rate nozzle was thinner than that of the conventional one. Numerically, the reduction of about 10% in coating thickness for the present condition can be materialized.

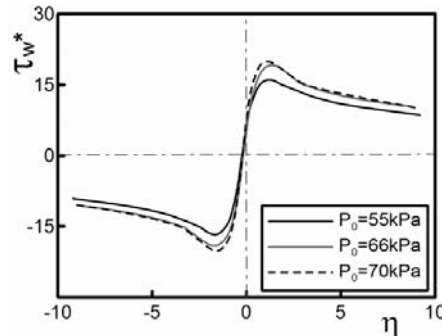
In other words, this means that it is possible to reduce the stagnation chamber pressure of the nozzle to obtain the same coating thickness compared with the case of the conventional nozzle.

As a consequence, it results in the decreases of harmful splashing problems and energy consumption levels to some extent.

Fig. 10 shows the effects of stagnation settling chamber pressure on the coating thickness for the case of the constant expansion rate nozzle of 3.0 m/s.



(a) Non-dimensional pressure gradient with p_0 ($H=1.0 \text{ mm}$, $S=10 \text{ mm}$, $V_s=3.0 \text{ m/s}$)



(b) Non-dimensional wall shear stress with p_0 ($H=1.0 \text{ mm}$, $S=10 \text{ mm}$, $V_s=3.0 \text{ m/s}$)

Fig. 8. Effect of p_0 on characteristics of wiping jet for $\dot{p}=88,000 \text{ s}^{-1}$.

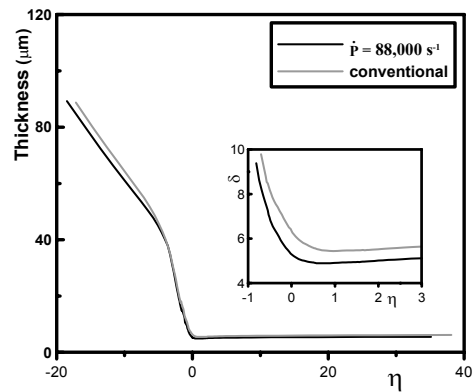


Fig. 9. Comparison of the coating thickness between constant expansion rate nozzle and conventional one ($H=1.0 \text{ mm}$, $S=10 \text{ mm}$, $p_0=66 \text{ kPa}$, $V_s=3.0 \text{ m/s}$).

For the same strip speed, the coating thickness is thinning with an increase of p_0 due to the increases of shear stress and impinging wall pressure gradient.

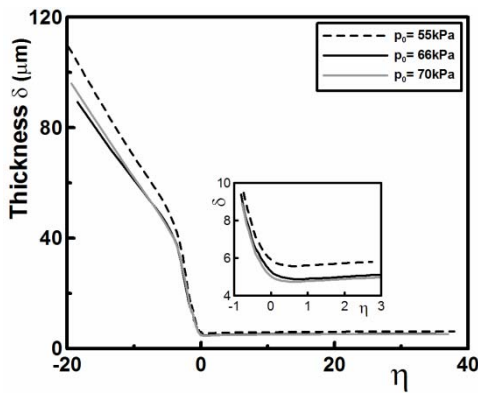


Fig. 10. Coating thickness with p_0 for $\dot{p}=88,000 \text{ s}^{-1}$ ($H=1.0 \text{ mm}$, $S=10 \text{ mm}$, $V_s=3.0 \text{ m/s}$).

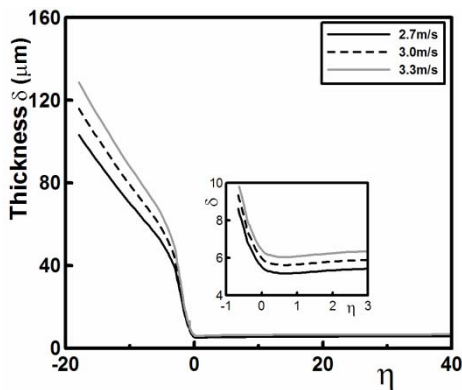


Fig. 11. Coating thickness with V_s for $\dot{p}=88,000 \text{ s}^{-1}$ ($H=1.0 \text{ mm}$, $S=10 \text{ mm}$, $p_0=66 \text{ kPa}$).

Especially, since the effect of shear stress acting at the interface between the zinc liquid film and the impinging jet is more dominant than the gravitational effect, the position of the minimum coating thickness is located at the slight upstream of the origin.

Finally, the effect of strip speed on the coating thickness is shown in Fig. 11. For the case of the same coating conditions excepting the strip speed, since the larger the strip speed is, the less the influx of impinging momentum per unit area of strip, the coating thickness is thickened in proportion to the increase of strip speed.

5. Conclusions

In order to clarify the jet structure issuing from a constant expansion rate nozzle for hot-dip galvanizing process, the impinging wall shear stress, the impinging wall pressure gradient and the coating film thickness with p_0 and V_s are obtained. And, the results can

be summarized as follows.

- (1) From the viewpoint of energy saving, it is advisable to use a constant expansion rate nozzle. It turns out that the coating thickness for $\dot{p}=88,000 \text{ s}^{-1}$ for the same $p_0=66 \text{ kPa}$ and $V_s=3.0 \text{ m/s}$ is 10% thinner than that case for the conventional one.
- (2) The minimum coating thickness is positioned at the slight upstream $\eta \approx 0.3$ of the origin.

Nomenclature

- b : Half-width of impinging pressure distribution (mm)
- g : Acceleration of gravity (m/s^2)
- H : Nozzle slot height (mm)
- L_{pc} : Potential core length (mm)
- p_i : Impinging pressure (kPa)
- p_0 : Plenum chamber pressure (kPa)
- p_s : Maximum impinging pressure (kPa)
- \dot{p} : Expansion rate ($\equiv -\frac{1}{p} \frac{dp}{dt}$) (s^{-1})
- q : Volume flow rate per unit width of strip (m^2/s)
- S : Gap between nozzle lip and strip (mm)
- t : Time (s)
- u : Velocity in x direction (m/s)
- V_s : Strip speed (m/s)
- x : Vertical coordinates (mm)
- y : Horizontal coordinates (mm)
- δ : Coating thickness (mm)
- η : Non-dimensional x coordinate ($\equiv x/b$)
- μ_l : Dynamic viscosity of liquid zinc ($\text{Pa} \cdot \text{s}$)
- ρ_l : Density of liquid zinc (kg/m^3)
- τ_w : Wall shear stress (N/m^2)

References

- [1] J. J. Butler, D. J. Beam and J. C. Hawkins, The Development of Air Coating Control for Continuous Strip Galvanizing, *Iron and Steel Engineers*, 47 (2) (1970) 77-86.
- [2] J. A. Thornton and H. F. Graff, An Analytical Description of the Jet Finishing Process for Hot-dip Metallic Coatings on Strip, *Metallurgical and Materials Transactions B*, 7 (4) (1976) 607-618.
- [3] M. Dubois, J. M. Buchlin, A. Gosset and V. Perrot, Effect of Nozzle Tilting on Splashing in Jet Wiping, *Galvatech'04 Conference Proceedings*, (2004) 197-206.
- [4] M. Dubois, M. L. Riethmuller, J. M. Buchlin and M.

- Arnalsteen, The Gas-Jet Wiping Limit: The Splashing Phenomenon, *Galvatech'95 Conference Proceedings*, (1995) 667-673.
- [5] T. Hara, T. Adaniya, M. Yamashita, Y. Tajiri and M. Ogawa, Development of a New Gas Wiping Process for High-Speed Chemical Treatment, *Iron and Steel*, 105 (1984) 90-97.
- [6] M. J. Moore and C. H. Sieverding, Two-Phase Steam Flow in Turbines and Separators, *McGraw-Hill Book Co.*, (1976) 127-140.
- [7] C. V. Tu and D. H. Wood, Wall Pressure and Shear Stress Measurements Beneath an Impinging Jet, *Experimental Thermal and Fluid Science*, 13 (1996) 365-373.
- [8] C. H. Ellen and C. V. Tu, Dec. An Analysis of Jet Stripping of Liquid Coatings, *Journal of Fluids Engineering*, 106 (1984) 399-404.
- [9] Y. Takeishi, A. Yamauchi and S. Miyauchi, Gas Wiping Mechanism in Hot-dip Coating Process, *Iron and Steel*, 81 (6) (1995) 643-648.
- [10] N. Trentacoste and P. M. Sforza, Further Experimental Results for Three-dimensional Free Jets, *AIAA*, 5 (1967) 855-891.



Soon-Bum Kwon received his B.S. and M.S. in Mechanical Engineering from Kyungpook National University in 1974 and 1980, respectively. Then he received his Ph.D. from Kyushu University in 1987. Now he is a Professor at the School of Mechanical Engineering at Kyungpook National University. His research interests are compressible gas dynamics and nonequilibrium condensation.